SSRG International Journal of Electrical and Electronics Engineering
ISSN: 2348-8379/ https://doi.org/10.14445/23488379/IJEEE-V12I8P118

Volume 12 Issue 8, 196-213, August 2025

Original Article

Enhancement of Power Quality with Hybrid Renewable Energy Systems Using STATCOM

Amit Kumar[1*] Jayanti Choudhary[2]

[1*,2]*Research Scholar, Department of Electrical Engineering, NIT Patna, India.*

[1]*Corresponding Author : amitk.phd19.ee@nitp.ac.in*

Received: 12 June 2025 Revised: 14 July 2025 Accepted: 13 August 2025 Published: 30 August 2025

Abstract - *To address Power Quality (PQ) concerns like voltage sag, swells, harmonics, and fluctuations, this paper explores the incorporation of a Static Synchronous Compensator (STATCOM), a Hybrid Renewable Energy System (HRES) that comprises Photovoltaic (PV) panels, Battery Energy Storage Systems (BESS) and Fuel Cells (FC). These problems are common in systems that use renewable energy sources because of their erratic nature and reliance on the weather. The goal of the proposed solution is to use STATCOM to enhance voltage stability and reactive power compensation optimization. This is accomplished by utilizing a hybrid approach that combines the Harris Hawks Optimization (HHO) algorithm and Recurrent Neural Networks (RNN) to enhance the gain parameters of the PID controllers within the STATCOM control circuit. MATLAB/Simulink 2020Ra is used to implement this optimization, which is then tested on an IEEE 9 bus system. The proposed RNN-HHO technique is compared to standard algorithms like Whale Optimization Algorithm (WOA) and Elephant Herding Optimization (EHO) using metrics such as Total Harmonics Distortion, voltage sag, swell, fluctuation, cost, and power loss.*

Keywords - *HRES, STATCOM, Power quality, THD, IEEE 9 bus system.*

1. Introduction

The three stages of power systems are typically referred to as distribution, transmission, and generation. Synchronous generators are frequently used in the first stage, known as generation, to produce electricity [1]. Subsequently, transformers broaden their voltage range before power transfer to lower line voltage and current, minimizing power transfer losses. After transmission, voltage is stepped down using transformers to ensure proper distribution [2]. Power systems aim to provide constant power while preserving voltage stability. Rising living standards, industrialization, and urbanization all increase power demand and utility burdens [3]. The world's power needs cannot be satisfied by conventional power sources, which creates problems for electricity security and stability. The enormous amounts of pollutants also present serious environmental risks [4]. Renewable and Distributed Energy Resources (DER) have supplanted conventional energy sources in recent decades. Utility engineers view DERs as a workable approach to satisfying load demand and efficiently resolving power issues [5]. Renewable Energy Sources (RES) are becoming increasingly significant in the modern world because conventional sources negatively affect the environment. RES are more effective at reducing pollution and global warming [6]. The growing importance of Distributed Generation (DG) based on RES is attributed to advancements in innovation and environmental awareness. DG based on HRES is the most recent advancement in the renewable energy system, demonstrating high performance and reliability [7]. Increased WT and PV reproductive technologies enable the utilization of rapidly expanding RES, the primary objective of which is lowering program costs. Furthermore, it could be contended that solar photovoltaic and wind turbine technology configurations are the most widely implemented and integrated technologies [8]. Utilizing multiple alternative energy sources simultaneously makes hybrid renewable energy technologies popular as a means of producing electricity. At the moment, RES like wind and PV are regarded as encouraging; however, PV energy is given more weight due to its significant cost reduction [9]. As more renewable power is produced and more nonlinear demands are placed on the system, power quality has grown to be a major concern [10]. The main source of this issue is the utilization of nonlinear power electronic strategies, which cause frequency distortions in the grid and change the sinusoidal form of the supply [11]. Coupling the outcome of these RESs to the power grid employing DC-AC inverters is necessary. PQ drawbacks like voltage sags and swells, harmonics, and other problems are encountered through the power electrical gadgets linking diverse RES connected to the grid [12]. Modular devices known as FACTS, or flexible AC transmission systems, are combined into the entire technique to develop system performance and support the power factor. For FACTS devices, there are three different sorts of network interfaces:

parallel, series, and a blend of parallel and series. All three of these categories have unique uses and characteristics that must be defined and regulated before being included in the scheme [13]. During sag/swell voltage conditions, shunt forms share reactive power in conjunction with the system to keep the voltage constant. Shunt compensators, such as Thyristor Controlled Reactor (TCR), Distribution STATACOM (DSTATCOM), and Static Compensators (STATCOM), were used to enhance the relationship of some RESs to the grid. Static synchronous compensators, or STATCOMs, are shunt FACTS devices that are extensively employed in voltage regulation and strength functions at the common coupling point (PCC). They used to offset voltage imbalances [14].

The STATCOM device adjusts reactive power volume to adjust the voltage at the PCC. Power is generated by the STATCOM. That is reactive to raise the voltage of the grid when it is below the required level. Conversely, if the system's voltage is higher than expected, it uses the proper quantity of power that is reactive to lower the voltage [15]. Most on-statcom controls often perform poorly in operational practice due to slow convergence, local optimization, and difficulty in adapting to various repeatable phenomena. A research gap exists for a formal, advanced, predictive, and optimization-driven system. The current research proposes a hybridization between a current neural network for predictive PQ modeling and a Harris Hawk Optimization (HHO) tuned PID controller.

The following are the work's principal contributions:

- Enhancing PQ and voltage stability while combining the benefits of time-series learning and effective optimization is possible with this innovative method of integrating RNN and HHO for optimizing STATCOM's PID controller parameters.
- The application of STATCOM for reactive power compensation in an HRES shows an effective method of controlling intermittent RES, which improves voltage stability and reduces PQ disturbances.
- The effectiveness of the suggested RNN-HHO-based command strategy is established by the considerable improvements in lowering THD and stabilizing voltage that are observed when it is extensively verified on a system using IEEE 9 buses and contrasted with alternative algorithms.

2. Literature Survey

Researchers presented several strategies to address PQ problems combined with STATCOM devices. This section reviewed the PQ mitigation that was implemented in an effort to lessen the problem.

Prasad et al [16] have estimated the load current values for weight via an innovative control technique. AI is suggested for shunt compensators. The conjunction of the load currents and an input signal property forms the basis of the control strategy. An ANN (Artificial Neural Network) -based STATCOM prototype is executed employing VSC and a PWM controller approach utilizing an AI control process designed in MATLAB/Simulink. This suggests that the AI-based STATCOM controller outperforms the conventional controller based on these results.

Ram et al [17] have created an enhanced adaptive command structure on A generalized second-order integrator (U-SOGI) in order to DSTATCOM. A damping factor, three mathematical operators, two integrators, and a structure comprise this structure, resulting in the proposed method for control being less complicated than transformation-based methods. The basic reactive and active mechanisms of the distorted load current are extracted via this control algorithm. These elements are further multiplied by the appropriate voltage templates to generate the currents of reference. Furthermore, the damping element is attuned to lower the DC offset and lessen the periodicity in the mass element under temporary circumstances.

Kumar, et al [18] have controlled both SPV-wind energy sources using Observe and Perturb (P&O) style Maximum Power Point Tracking (MPPT) method to optimize real output of power in a variety of environmental circumstances. Current and voltage controllers based on Proportional Integrals (PI) produce a modulating signal that varies sine-wise. The reactive power reimbursement goal is accomplished by connecting the D-STATCOM at the PCC. Its use contributes to the maintenance of an effective power distribution system and a stable utility-grid connection. According to IEEE-519 standards, simulation studies demonstrate that harmonics are less than 5% and decrease at various coupling points.

Bajaj et al. [19] suggested the Analytic Hierarchy Process (AHP) for the PQ evaluation of distorted systems about Distributed Generation (DGs) based on RES. The suggested method of evaluating PQ involves creating a Unified Power Quality Index (UPQI) to evaluate the PQ results of each bus in the system, taking into consideration four Voltage phenomena in PQ unbalance, harmonics, sags, and steady-state voltage profile. The utility of the procedure accessible here is demonstrated by applying it to an altered IEEE 13 system of buses in the Simulink/MATLAB environment.

Adware and Chandrakar [20] have examined two distinct FACTS devices, the SVC and the STATCOM, and suggested an innovative controller for fuzzy logic to lessen the impact of PQ concerns. The purpose of the controller for fuzzy logic is to raise the calibre of power by acting as a voltage manager. Extensive analysis was conducted to examine how, in a Multi-Terminal Load (MTL), two controllers structured wind turbines successfully mitigated voltage swell/sag, improved reactive and active strength, and controlled flickering voltage.

Sindi et al [21] have presented a creative connectivity between multiple microgrids using specific compensatory Low-inertia device schemes to improve voltage profiles and reduce harmonics by applying power compensation strategies. An Adaptive PQ Compensator (APQC) comprising shunt and series reactors is the compensation mechanism in use. Furthermore, the most recent puzzle optimization algorithm, Swarm intelligence-based, is utilized to obtain the top-rated PID controller gains for self-correction, exposing the typology of APQC. The effectiveness of the multilevel mechanism approach in the presented APQC was evaluated using MATLAB/Simulink.

Hasanzadeh et al [22] have suggested that to enhance the one-cycle controller's performance, a new structure is needed. STATCOM uses a three-level inverter structure, which has advantages over a two-level structure in terms of harmonic reduction and losses. The switching has been controlled using the STATCOM compensator's one-cycle control method. Voltage swells, sag, harmonics, and brief outages are among the improvements. The multilevel STATCOM is also assessed and contrasted with standard PWM to show the effectiveness of the suggested manager.

Goud et al [23] have provided that DPFC, or distributed power flow controller, is a versatile tool to alleviate certain power quality problems, such as harmonic elimination in a System of Hybrid Power (HPS) and voltage sag and swell. The wind, BESS, and PV systems make up the HPS described in this work. To resolve the PQ challenges facing HRES schemes, Optimization of Black Widows (BWO) DPFC-PQ, or DPFC real and reactive power, is consequently developed. The DPFC-PQ is powered by FOPID, or fractional-order PID, controller that was augmented via the BWO approach.

Zanib et al [24] have recommended utilizing an ANN-driven UPQC in order to increase PQ of a network with low voltage linked to a system of hybrid DG. An extensive performance evaluation of a DG system incorporating a PV and wind power through a PI controller and an ANN controller is the primary objective of the recommended work. This is done through the use of a power quality conditioner that is unified (UPQC). The suggested ANN aims to provide better dynamic and steady state performance than the PID controller. Goud et al [25] have described the addition of RES to the grid, like PV, wind, and batteries. Grey Wolf Optimization (GWO) and FOPI controllers are accustomed to maximize the tuning reduction of the Hybrid Shunt Active Power Filter (HSHAPF). Elimination. Harmonics are successfully decreased by adjusting the FOPI parameters via means of GWO. The THD has been effectively compensated by comparing the suggested prototype to the functioning power filter, a PI controller, the filter without any filter, the GWO-FOPI and the passive filter-based controller. Kamel et al [26] have suggested two kinds of optimization approaches to improve STATCOM's dynamic performance: Particle Swarm Optimization (PSO) and Ant Colony Optimization (ACO). To improve Data Monitoring dynamics, PSO and ACO seek to modify the coefficients of PI controllers. Consumer loads trip as a result of power quality issues related to voltage spikes and interruptions. The STATCOM's impact at PCC, the location of A wind farm under deep disturbances, is looked into. The PI authorities used to manage the performance of the STATCOM are tuned using five different techniques: FUZZY logic, ACO, classical PI, PSO, and hybrid PSO-ACO. The primary measures utilized to assess the efficacy of these techniques at the event of faults, in addition to the settling duration needed to reintroduce the system to a stable condition.

Peddiny et al [27] have frequently employed STATCOM to correct and compensate the power bus voltage level. The traditional PI-based controller has been replaced in this study with an ANN and GWO-based controlled STATCOM, which improves STATCOM performance overall. Its simplicity, flexibility, resilience, and capacity to consider the grid's non-linearities make the ANN controller the recommended choice. The classifier was trained offline using PI controller data. The efficiency of STATCOM was evaluated on a 25 km transmission line under three faults and an increased load using the MATLAB/Simulink software.

Mishra et al [28] have provided a hybrid PSO-GWO and FOPID Controller (FOPIDC) optimized HSAPF for reactive power and harmonic reimbursement. To reduce the harmonics, the method known as PSO-GWO is applied to regulate the FOPID controller's parameters. When contrasting active and passive filters, it is found that the latter is not affordable for a high rating, while the former is large and has an intricate design. Thus, by combining MATLAB/Simulink with an experimental real-time configuration, an integrated framework made up of a shunt passive and in-motion filter is established.

Moghassemi et al [29] have suggested enhancing the PQ of off-grid PV systems with a new Dynamic Voltage Restorer (DVR) fed by solar via Trans-Z-source Inverter (TransZSI). In response to a voltage disturbance, the PCC injects the desired voltage using a power electronic compensator, or DVR. TransZSI is employed instead of conventional VSI in the suggested DVR because it offers better buck/boost, a greater gain from the voltage boost range, smaller passive elements, and less voltage stress.

Bilgundi et al [30] have emphasized the significance of taking into account the effects of a nonlinear load, frequency variation, and distortion of grid voltage when developing and implementing a controller for PQ restoration. The suggested controller has the added benefit of enhancing grid PQ, providing energy to nearby loads, and transferring excess DG electricity to the grid. To improve PQ, a DG and an ANFIS-centred PI current regulator are suggested. Since no additional

hardware is needed, the method is inexpensive. To verify the efficacy of the suggested controller, outcomes are contrasted with fuzzy, PI-RC, and PI current controllers.

Alwaeli et.al [31] suggest a clever method to maximize grid electricity quality-based mixed power systems that make use of wind and solar power. STATCOMs, or Static Synchronous Compensators, are used to improve renewable energy incorporation. The Grey Wolf Optimization (GWO) algorithm improves control parameters and system reliability. The strategy shows improved stability during voltage and current fluctuations, effective reactive power generation, and stable PCC during faults.

Slimene [32] suggests a hybrid RES design that uses sophisticated control techniques to boost system efficiency. Energy storage systems, fault current limiters, and flexible AC transmission systems are among the technologies included in the framework. Simulation results show the approach enhances fault resilience, grid stability, and power quality, outperforming EN 50,160 and IEEE 519 standards. This research offers a solid remedy for a sustainable energy future.

Table 1. Comparison of the existing paper

Author(s)	Method Used	Advantages	Disadvantages
Prasad et al. [16]	ANN-based STATCOM PWM	High accuracy, AI-based adaptability	Complex training, implementation effort
Ram et al. [17]	U-SOGI adaptive control for DSTATCOM	Simpler than transformation methods, good transient response	May struggle with nonlinear, fast-varying loads
Kumar et al. [18]	PI control P&O MPPT and DSTATCOM	Improved real power output, <5% harmonics	Sensitive to environmental changes, PI tuning needed
Bajaj et al. [19]	AHP for PQ UPQI in DG systems	Multi-criteria PQ evaluation, simulation-based	Limited to modelled scenarios, subjective weighting
Adware & Chandrakar [20]	Fuzzy logic SVC & STATCOM	Effective PQ improvement, voltage control	Rule-based complexity, tuning needed
Sindi et al. [21]	APQC swarm-based PID tuning	Strong harmonic mitigation, self-tuning	High computational load for optimization
Hasanzadeh et al. [22]	One-cycle control 3-level STATCOM	Better harmonic suppression, lower losses	Complex multilevel inverter design
Goud et al. [23]	DPFC-PQ FOPID and BWO	Improved PQ in HPS, optimized control	Complex control logic, tuning challenges
Zanib et al. [24]	ANN-based UPQC	Enhanced dynamic and steady-state performance	Requires ANN training, data dependency
Goud et al. [25]	HSHAPF GWO-FOPI	THD was effectively reduced, better than PI	Complex optimization, real-time application difficulty
Kamel et al. [26]	PSO & ACO tuned PI in STATCOM	Fast fault recovery, reduced overshoot	Metaheuristics may need high computation
Peddiny et al. [27]	ANN + GWO-based STATCOM	Robust and nonlinear grid handling	ANN complexity, training needs
Mishra et al. [28]	PSO-GWO tuned FOPIDC for HSAPF	Hybrid filtering, improved harmonic compensation	Larger structure, difficult real-time control
Moghassemi et al. [29]	DVR TransZSI	Better voltage gain, compact design	Circuit complexity needs control precision
Bilgundi et al. [30]	ANFIS-PI controller for DG	Low cost, adaptive, enhances grid PQ	ANFIS training complexity, data reliance
Alwaeli et al. [31]	GWO + STATCOM	Better power quality & system reliability	Limited to control; hardware not addressed
Slimene [32]	Hybrid RES + FACTS + Storage	High stability & fault resilience	Complex and costly setup

Advanced control approaches like ANN, FOPID, PSO, ACO, FLC, and hybrid metaheuristic algorithms have been applied to compensation systems, but they often face challenges such as computational complexity, accuracy, and scalability.

These methods are not suitable for grid-connected situations. To overcome these issues, the research focuses on developing low-level complexity AI models that achieve scalability, self-tuning, and PQ control capabilities for modern distributed energy resource-based local situational awareness.

2.1. Problem Statement

The addition of RES, such as wind and PV, may cause voltage fluctuations and harmonics in microgrid systems. These problems hinder the performance of delicate equipment and lower the system's overall efficiency. The primary objective of this research is to develop a preventative method for a STATCOM that efficiently controls voltage and supports reactive power for an HRES-based microgrid, enhancing its power quality.

A power electronic converter integrates the microgrid's various RES, like solar fuel cells, as well as energy storage, with the main grid. Additional PQ problems, such as variations in voltage and harmonics, may arise from the incorporation of energy storage devices. As a result, developing a STATCOM control strategy that successfully offsets these power quality problems is crucial.

3. Proposed Methodology

In the proposed work, a HRES consisting of FC, BESS, and PV panels is the subject of a proposed methodology aimed at addressing PQ deficiencies. PQ issues like voltage harmonics, swells, fluctuations, and sags result from these systems' inherent variability and dependence on weather. The study incorporates a STATCOM for reactive power compensation to address these difficulties. The key contribution of this work is the hybrid algorithm, which blends HHO and RNN to improve the gain parameters of the STATCOM. The goal is to improve system response and voltage stability under various HRES conditions. Using MATLAB/Simulink 2020Ra to model the HRES and STATCOM, then applying the best control strategy to an IEEE 9-bus architecture, is the methodology. Figure 1 illustrates the overall proposed methodology of the work.

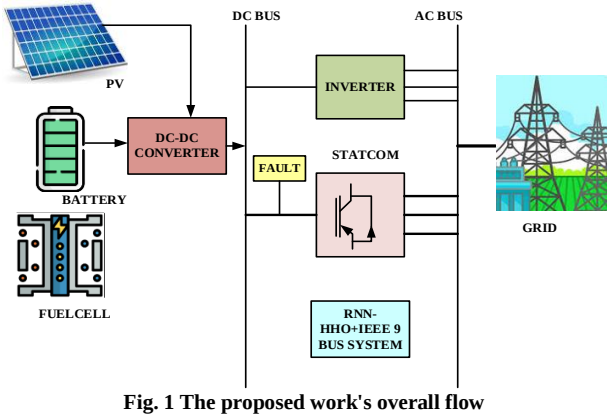

Fig. 1 The proposed work's overall flow

3.1. Equivalent Structure of PV Model

PV is the best substitute for using solar energy to generate electricity without producing greenhouse gases. It has a long lifespan, good efficiency, low maintenance, and sturdiness among the many renewable resources. The PV system consists of series-connected cells that generate the required voltage. The PV plane of the ultimate voltage of the output estimate is produced by doubling the voltage at the terminal by the current that is produced. In Figure 2, the PV built model is shown.

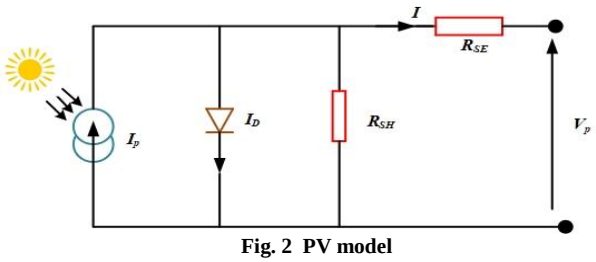

Fig. 2 PV model

The PV panel terminal and current voltage for design are calculated using Equations (1) and (2).

$$I_p = I_{SC} - I_O\left\{\exp\left[\frac{Q}{akt}\left(V_p + I_p R_{SE}\right) - 1\right]\right\} - \frac{V_p + I_{SC}R_{SE}}{R_{SH}} \quad (1)$$

$$V_p = \frac{akt}{Q}\ln\left\{\frac{I_{SC}}{I_p} + 1\right\} \quad (2)$$

Where Q is an electron's charge, t is the Kelvin temperature. k is the diode ideality component and Boltzmann's constant, R_{SH} and R_{SE} Are the resistances in series and shunt? V_p Is the cell voltage, and I_{SC} Is the present. The strength produced by the PV is computed as (3)

$$P_{PV}(t) = N_{pv}(t) \times I_{pv}(t) \times V_{pv}(t) \quad (3)$$

Where $V_{pv}(t)$ is the PV voltage, $N_{pv}(t)$ is the quantity of cells. In the PV array, $I_{pv}(t)$is the PV current, and. P_{PV} Is the PV power?

3.2. Battery Energy Storage System (BESS)

The BESS is an extra energy storage source, which is necessary as PV and FC together are sometimes not enough to fulfil the demand for the burden. The one that chooses and models the typical BESS model is as follows:

$$V_{BAT} = E - R_b.I_{BAT} \quad (4)$$

$$E = E_0 - K.\frac{Q}{Q - k.\int i_1 dt} + A.exp(-B.\int i_1 dt) \quad (5)$$

$$SOC(\%) = 100\left(1 - \frac{Q_d}{C_{BAT}}\right) = 100\left(1 - \frac{I_{BAT}}{C_{BAT}}\,t\right) \quad (6)$$

Where BESS voltage, stored current hour, internal capacity, and current are represented, correspondingly, by V_{BAT}, Q_d, C_{BAT} and I_{BAT} . The crucial variables that must be managed are the BESS SOC and the electricity saved during charging. The Simulink prototype of the battery is illustrated in Figure 3.

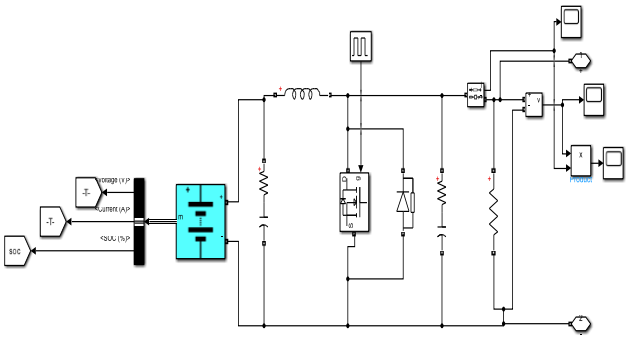

Fig. 3 Battery model in simulink

3.3. Modelling of FC

The physical and electrochemical processes inside an FC are mathematically signified by several equations. The Nernst equation is frequently used. It links the temperature (t), the proportion of reactant to product concentrations (q), and the voltage of the cell (F_{cell}) to the normal potential of cells (F_0) in the following ways:

$$F_{cell} = F_0 - \left(\frac{RT}{nf}\right) * lnq \tag{7}$$

The symbol represents the Faraday constant f, the temperature in Kelvin is denoted by T, the quantity of electrons exchanged throughout the electrochemical process is signified by n, and the gas constant is denoted by R.

$$I = I_O \left[Exp\left(\alpha nf \frac{\eta}{RT}\right) - Exp\left(\alpha nf \frac{\eta}{RT}\right)\right] \tag{8}$$

For fuel cell modelling, another essential calculation is the electrochemical kinetics described by the Butler–Volmer equation. Process at the electrodes. The density of current (I_o), transfer coefficient (a), and overpotential (h) are related by Equation (8). The current density is represented by I, and the difference between the equilibrium potential and the electrode potential of the electrochemical reaction is called h.

3.4. STATCOM

The PCC voltage regulates STATCOM, a static shunt compensator with an inductive and capacitive output current. Figure 4 displays the STATCOM control block diagram.

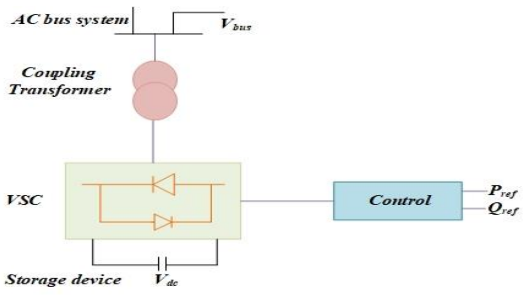

Fig. 4 STATCOM Device

The components of STATCOM include a coupling transformer, a VSC that is switched to the electrical grid at PCC, and a DC capacitive storage device for power. Equipped with the frequency of the AC power structure, the VSC produces a variety of regulated voltages. In the event that the PCC voltage amplitude drops, STATCOM produces reactive power (capacitive mode) and infuses a leading current into the grid at PCC. The term "lagging current" refers to the introduction of current from PCC's STATCOM to the grid while the device is operating in the inductive mode.

Consequently, when the PCC rises, the STATCOM captures the reactive power. Power exchange does not occur if the PCC voltage remains unchanged. This control inserted current from STATCOM suppresses fluctuations in PCC voltage during fault events. Figure 4 shows the Simulink model of STATCOM. There are two types of STATCOMs: converters for Voltage Sources (VSC) and Current Sources (CSC).

Since VSCs are typically more effective than CSC methodology, STATCOM uses VSCs. Assuming that the grid's electricity transfer route to STATCOM is positive and that $X_s"R_s$, The power that is active P as well as reactive power Q to the equations of STATCOM (9) and (10) clearly show that the P and Q are pushed through the output voltage variation V_s as well as the phase difference α between V_s and V_s.

$$P = \frac{V_S V_S^i sin\alpha}{X_s} \tag{9}$$

$$Q = \frac{V_S^i (V_S cos\alpha - V_S^i)}{X_s} \tag{10}$$

3.4.1. Control Strategy for STATCOM

The proposed control method is used to raise the PQ of a grid-connected framework by injecting reactive and real power.

3.4.2. Grid Voltages and Currents

Analysis of the Grid's Current and voltage is essential for PQ crises. The voltage and current of the 3-ϕ are adjusted to $\alpha\beta 0$ $(abc \rightarrow \alpha\beta 0)$.

$$V_a = V_m \sin(wt) \tag{11}$$

$$V_b = V_m \sin\left(wt - \frac{2\pi}{3}\right) \tag{12}$$

$$V_c = V_m \sin\left(wt - \frac{4\pi}{3}\right) \tag{13}$$

The instantaneous load current,

$$I_{la} = \sum I_{lan} sin\{n * (wt) - \theta_{an}\} \tag{14}$$

$$I_{lb} = \sum I_{lbn} sin\left\{n * \left(wt - \frac{2\pi}{3}\right) - \theta_{bn}\right\} \quad (15)$$

$$I_{lc} = \sum I_{lcn} sin\left\{n * \left(wt - \frac{4\pi}{3}\right) - \theta_{cn}\right\} \quad (16)$$

The one that grid the voltage and currents were expressed below using the Clarke transformation,

$$\begin{bmatrix} V_a \\ V_b \end{bmatrix} = \sqrt{\frac{2}{3}} \begin{bmatrix} 1 & -\frac{1}{2} & -\frac{1}{2} \\ 0 & \frac{\sqrt{3}}{2} & -\frac{\sqrt{3}}{2} \end{bmatrix} \begin{bmatrix} V_a \\ V_b \\ V_c \end{bmatrix} \quad (17)$$

$$\begin{bmatrix} I_a \\ I_b \end{bmatrix} = \sqrt{\frac{2}{3}} \begin{bmatrix} 1 & -\frac{1}{2} & -\frac{1}{2} \\ 0 & \frac{\sqrt{3}}{2} & -\frac{\sqrt{3}}{2} \end{bmatrix} \begin{bmatrix} I_{la} \\ I_{lb} \\ I_{lc} \end{bmatrix} \quad (18)$$

Calculation of both reactive and active power,

$$P = V_\alpha I_\alpha + V_\beta I_\beta \quad (19)$$

$$Q = -V_\beta I_\alpha + V_\alpha I_\beta \quad (20)$$

The frame axes are α and β. STATCOM is needed to add a certain amount of reactive power to a grid-connected system, and the controller helps increase PQ.

3.5. RNN-HHO

The hybrid RNN-The HHO algorithm is employed to adjust the STATCOM's gain parameters to resolve PQ problems. These RNN and HHO approaches are elucidated in this section.

3.5.1. Harris Hawk Optimization Approach

The model for Hawk, Harris optimization. Was hunting going on? Strategies Harris hawks are among nature's more cunning birds. The Harris hawk initially employs an exploring strategy after spotting its prey before coming up with A plan of assault. HHO possesses stages for seeking strategy-based exploration and exploitation. When properly formulated, the population-based stochastic optimization method known as HHO is used to solve engineering issues.

Step 1: Initialization

Initializing the parameters is the first stage in HHO; This involves the PID controller's parameters, which are regarded as the input parameters.

Step 2: Generation at Random

Random vectors are produced for the input vectors after initialization.

Step 3: Fitness Evaluation

The fitness parameter establishes the desirable and unwanted solutions. Equation (21) is used to represent the fitness equation.

$$Fitness = \sum Min \quad (21)$$

Where Min is used to represent the minimisation of the error.

Step 4: Exploration phase

At this point, the exploring strategies of the Harris hawks are imitated. Harris hawks have strong eyes that see game, although they periodically fly over desert regions to observe for better hunting. This process is looping. The Harris Hawk points to the correct response in each loop's perfect hunting position.

$$k(u+1) = \begin{cases} k_{rand}(u) - e_1 |k_{rand}(u) - 2e_2 k(u)| v \geq 0.5 \\ \left(k_{Rabbit}(u) - k_c(u) - e_3\left(HQ + e_4(DQ - HQ)\right)\right) v < 0.5 \end{cases} \quad (22)$$

When Harris hawks are just roving, they adopt two separate exploration methods. These strategies are defined in Equation 22, where Q is the likelihood that a certain strategy will be employed, and x t 1 is a vector that depicts the Harris hawk's location during each iteration. The prey's location vector is represented by k_{Rabbit}, the hawk by x_t, and the random values within e_1, e_2, e_3, e_4, and $Q$are (0, 1). For $X_{mn}(t)$, the average location of the current hawk population, and $k_{rand}(u)$ A hawk selected at random from the estimate applies Equation 23.

$$X_{mn}(t) = \frac{1}{N}\sum_{i=1}^{N} X_i(t) \quad (23)$$

Step 5: Change from exploration to exploitation

The algorithm mimics the second phase of hunting by Harris's hawks, during which they alter their movements in response to the greater energy (E) of the prey they are pursuing. The "transition stage" refers to this phase. The model is illustrated in Equation (24), where $E_\emptyset$ is the starting vitality level of the prey and t_{mn} Is the extreme quantity of iterations. In the exploration stage of the algorithm, the variable $|E| \geq 1$ is searched for optimal solutions, and in the exploitation step, the solutions identified in the variable $|E| < 1$ are improved.

$$E = 2E_\emptyset \left(1 - \frac{t}{t_{mn}}\right) \quad (24)$$

Step 6: Exploitation phase

The Harris' hawk's last phase of hunting comprises a variety of tactics that consider the prey's level of energy as well as its ability to escape. These elements are carefully taken into account to increase the odds of a successful hunt for the hawks. Accepting X as the probability of the prey, where (W) denotes a successful escape and (T) denotes a failed escape. Accepting r as the likelihood of the prey, where $r < 0.5$ indicates a successful escape and $r \geq 0.5$ indicates a failure

to escape. For scenarios $r \geq 0.5$ and $|\mathrm{E}| \geq 0.5$, a mild siege, which is defined in Equation (22), will be applied.

$$X(\mathrm{T}+1) = \Delta X(\mathrm{T}) - \mathrm{E}\left|JSX_{prey}(\mathrm{T}) - X(\mathrm{T})\right| \quad (25)$$

$$\Delta X(\mathrm{T}) = X_{prey}(\mathrm{T}) + X(\mathrm{T}) \quad (26)$$

The variable represents the separation between the target's position and the locating agent's present position in Equation (25). $\Delta X(\mathrm{T})$. The target's capacity for arbitrary jumps, denoted by the term $JS(JS = 2(1 - \mathrm{r}_5))$, is established by the value of the arbitrary number r_5, which falls between the range of (0,1). The search agent will begin a harsh siege approach to exploit prey that has run out of energy under certain conditions. $r \geq 0.5$ and $|\mathrm{E}| < 0.5$ are met. Equation (24) provides a mathematical expression for this particular substage.

$$X(\mathrm{T}+1) = X_{prey}(\mathrm{T}) - \mathrm{E}|\Delta X(\mathrm{T})| \quad (27)$$

The presence of sufficient energy will create a slow, quick dive, a soft siege if $r < 0.5$ and $|\mathrm{E}| \geq 0.5$ is both greater than 0.5. In this case, the next step is predicted by the equations (25) and (26), where D, S, and $LF(D)$ stand for dimension, a Levy flight function, and a random vector of size 1D, respectively. As a result, the position is updated using Equation (28).

$$\mathrm{Y}_1 = X_{prey}(\mathrm{T}) - \mathrm{E}\left|JSX_{prey}(\mathrm{T}) - X(\mathrm{T})\right| \quad (28)$$

$$\mathrm{Z}_1 = \mathrm{Y}_1 + \mathrm{S} \times \mathrm{LF(D)} \quad (29)$$

$$X(\mathrm{T}+1) = \begin{cases} \mathrm{Y}_1 & if\ F(\mathrm{Y}_1) < F(X(\mathrm{T})) \\ \mathrm{Z}_1 & if\ F(\mathrm{Z}_1) < F(X(\mathrm{T})) \end{cases} \quad (30)$$

The final substage of the hunting process, known as the "hard besiege progressive rapid dive," will be reached by the search agent when both. r and $|\mathrm{E}|$ have values that are smaller than 0.5. This step's mathematical representation is provided by Equation (31).

$$X(\mathrm{T}+1) = \begin{cases} \mathrm{Y}_2 & if\ F(\mathrm{Y}_2) < F\left(X(\mathrm{T})\right) \\ \mathrm{Z}_2 & if\ F(\mathrm{Z}_2) < F\left(X(\mathrm{T})\right) \end{cases} \quad (31)$$

Using Eqs. (32) and (33), respectively, Y_2 and Z_2 are determined.

$$\mathrm{Y}_2 = X_{prey}(\mathrm{T}) - \mathrm{E}\left|JSX_{prey}(\mathrm{T}) - X(\mathrm{T})\right| \quad (32)$$

$$\mathrm{Z}_2 = \mathrm{Y}_2 + \mathrm{S} \times \mathrm{LF(D)} \quad (33)$$

Step 7: Return the Solution's Best Position

Step 8: Termination

Check the termination requirements. Terminate the operation if the termination requirements are met after the maximum permitted repetitions. Once the above procedure is completed, the completed training dataset is employed to instruct the RNN, at which point the HHO is prepared to supply the training data, which is the final updated location value for the RNN.

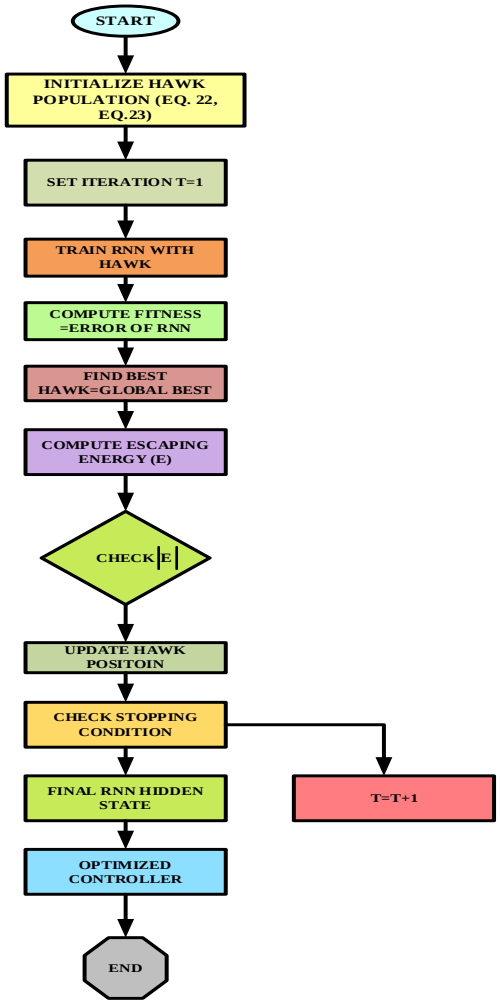

Fig. 5 Flowchart

3.6. RNN

RNNs are a specific type in which the output from one stage serves as the input for the subsequent stage. Unlike conventional neural networks (NNs), RNNs possess an obscure layer that enables them to remember data from prior steps in the process. This hidden state acts as a recollection, holding onto information from previous computations. Because RNNs employ similar biases and weights for all inputs, they simplify parameter growth and require less memorization than other types of neural networks. Thus, all three layers are combined into a single recurrent layer, and the strengths and biases of each hidden level will be the same. RNNs frequently experience "vanishing gradients" and

"expanding gradients." The size or inclination of the error curve's gradient drop determines the classification of these issues. One approach to solving these issues is simplifying the RNN model by lowering the neural network's hidden layer count. The hidden layers store the previous output of the hidden neuron and gather input from context neurons that are referred to as memory units. The PV's voltage, current, FC, and battery are the RNN's inputs in this paper. Each layer's fundamental procedure is taken into account. In this case, the RNN is being trained via supervised learning. The formula (34) is used to determine the status at the moment.

$$h_t = c(h_{t-1}, x_i) \tag{34}$$

Where in x_i Constitutes the state. of input, h_t is the existing situation, and h_{t-1} is the state that existed before.

The activation function ($tan\ f$) is applied using Equation (35).

$$h_t = tanf(W_{rn}h_{t-1} + W_{in}x_i \tag{35}$$

Where W_{in} Is what input the neuron and W_{rn} The recurrent neuron's output is computed using Equation (36).

$$o_t = (w_o.h_t) \tag{36}$$

Where the output layer is w_o, and o_t Is the output. It is possible to identify a learning computation that reduces error to zero. The following Equation (37) represents the work's objective function.

$$u(t) = k_p E(t) + k_i \int_0^t E(t)dt + k_d \frac{d}{dt}E(t) \tag{37}$$

The tuning parameters for the PID controller are shown in the STATCOM controller, and k_p, k_i and k_d.

Pseudocode for HHO-RNN

→ Initialize parameters
• Population size of hawks (N)
• Maximum iterations (T)
• Initialize random weights & biases of RNN as hawks' positions y_i Equation 22, Equation 23
→ While (t ≤ T iterations) do
For each hawk y_i :
• Train RNN weights/biases from hawk. y_i
• Compute fitness function = error of RNN.
→ Find the hawk with the highest level of fitness → set as rabbit (world-class RNN answer) Equation21
→ For each hawk y_i :
• Compute escaping energy E using Equation (24)
• If $\|E\| \geq 1$: (Stage of exploration)
• Revise the hawk position utilizing the Equation. (22-23)
• Else if $\|E\| < 1$: (Stage of exploitation)
• If $r \geq 0.5$ and $\|E\| \geq 0.5$: upgrade with Equation (25-26)
• Else if $r \geq 0.5$ and $\|E\| < 0.5$: upgrade with Equation (27)
• Else if $r < 0.5$ and $\|E\| \geq 0.5$: up ↓≥ using Equation (28-30)
• Else: update using Equation (31-33)
→ Replace the old hawk position with the updated position
→ Repeat until all hawks are updated
End
output

4. Results and Discussion

The effectiveness of the proposed methodology is examined and demonstrated in this section. HRES is being developed to address PQ issues and is connected to the grid. The proposed solution (RNN-HHO + IEEE 9) to address the PQ issues is to increase the system's stability via the controller. Battery, fuel cells, and photovoltaic systems are thought to be the primary sources for supplying the load demand. The proposed framework has been implemented employing MATLAB Simulink. The method is used with MATLAB/Simulink R2022a version and Windows 10 PRO. The Intel ® Core (TM) i3-6098P CPU @ 3.60 GHz is the processor being used, and there are 8 GB of RAM. PV, FC, and battery output, sag, swell, fluctuation, cost, power loss, and THD are among the performance metrics examined. The graphs are evaluated through an assortment of current methodologies, encompassing WOA and EHO. The Simulink Diagram for the proposed approach is displayed in Figure 6. The values of the parameters are shown in Table 2.

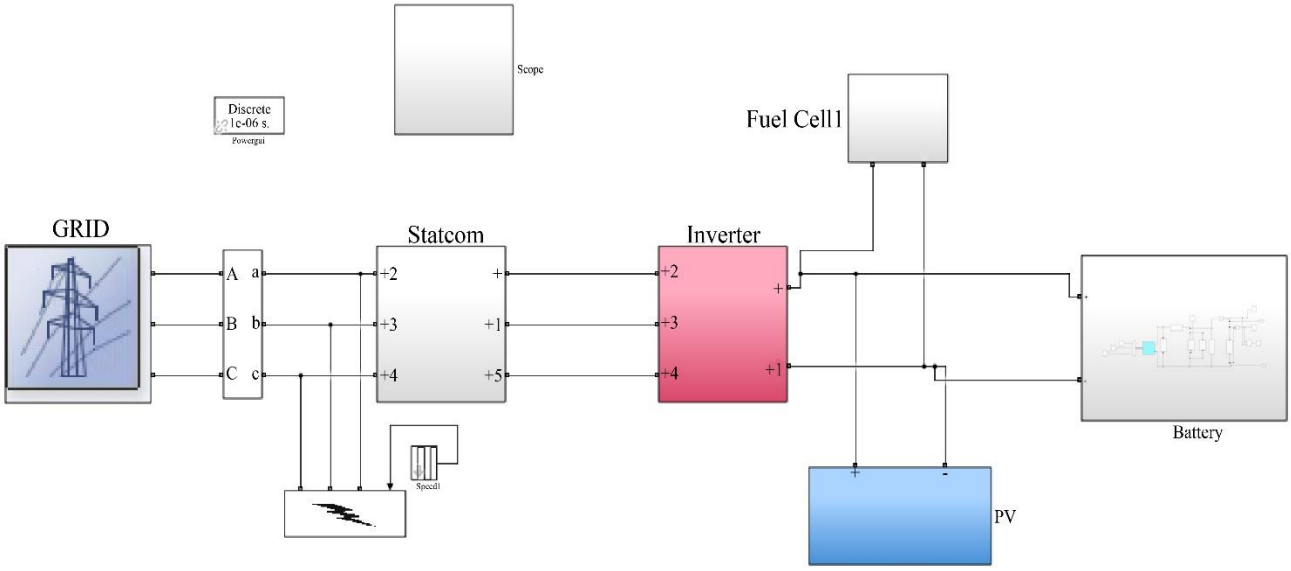

Fig. 6 Simulink diagram for the proposed method

Table 2. Simulink parameter values

S. No	Illustration	Specification	Rate
1	PV	Irradiance	3000 W/m^2
		Parallel Strings	40
		Temperature	25^O C
		Converter Resistance	50 Ω
		Series-Connected Modules per String	10
2	Battery	Rated Capacity	30 Ah
		Type	Lithium-Ion
		Battery Response Time	1 s
		Internal Resistance	0.147 Ω
		Nominal Voltage	440 V
		Initial SOC	100 %
3	Fuel cell	Maximum power	8325 W
		Nominal power	5998.5 W
		Air consumption	143.7 slpm
		Fuel consumption	60.38 slpm
4	DC link	capacitance	2200 μF
5	Grid	X/R ratio	7
		Frequency	60 Hz
		Phase-to-Phase Voltage	120 KV
6	Inverter	Snubber resistance	1 K Ω
		Carrier frequency	1000 Hz

4.1. IEEE 9 Bus System

One benchmark is the IEEE 9 bus system. A power framework is utilized for the power system evaluation and integrity investigation, utilizing parameters like load requirements, generator ratings, and line impedances. The system serves as a benchmark test scenario for numerous investigation projects and a vital resource for assessing how well power system stability and control techniques work. Researchers regularly use IEEE Bus Systems to test novel theories and concepts related to power production and distribution. This study investigates PQ issues using the IEEE 9 bus and FACTS devices, specifically the STATCOM. This bus system is simulated in MATLAB, and power flow, fuel cost, and power loss are examined using the STATCOM and RNN-HHO tuned STATCOM. This bus network that was used for this study has three generators on buses one, two, and

three; seven transmission lines that link the buses; nine bus bars; and three transformers, transformer number one situated between buses two and seven, transformer number two between buses nine and three, and transformer number three situated between buses one and four. In Figure 7, the IEEE 9 A bus system is shown.

Table 3. Line data for the IEEE 9 bus

From bus	To bus	R	X
1	4	0	0.0576
4	5	0.02	0.092
5	6	0.04	0.17
3	6	0	0.0586
6	7	0.01	0.1008
7	8	0.01	0.072
8	2	0	0.0625
8	9	0.03	0.161
9	4	0.01	0.085

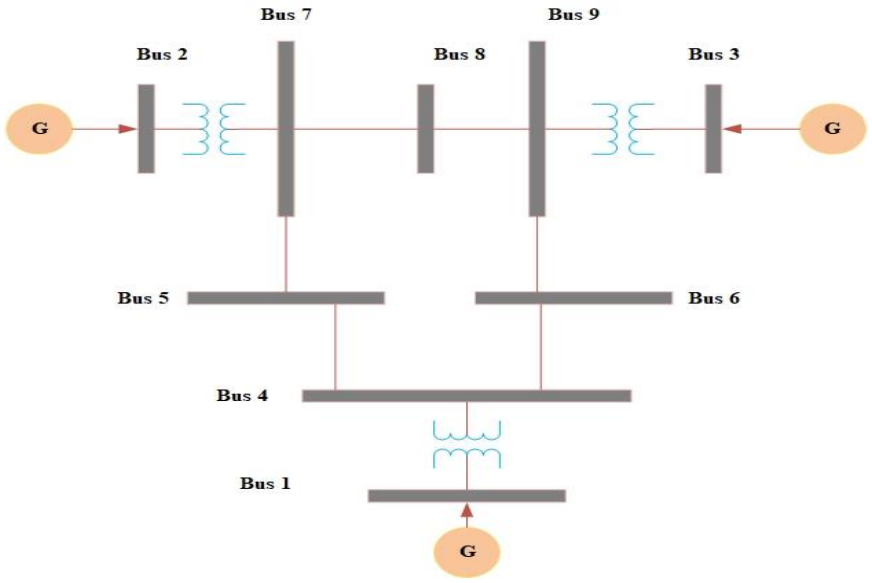

Fig. 7 IEEE 9 bus system

Three sources are taken into consideration in this simulation diagram: batteries, fuel cells, and photovoltaics. Initially, a converter is used to connect the battery, PV, and fuel cell in order to convert DC into DC voltage. The proposed controller receives DC voltage to control the system's voltage fluctuations. The regulated voltage is ultimately sent into the grid to satisfy the load demand.

The one that PV panel is supplied with an input of 1000 wb/m^2 of illumination and 25 °C of temperature. The lithium-ion type of battery used in the suggested approach has the following specifications: 440 V for nominal voltage, 30 Ah for rated capacity, 1 sec for response time, 0.14667 Ω for internal resistance, and 100% for initial SoC. An investigation of the PV power, voltage, and current is shown in Figure 8.

The output of a PV system voltage starts at 300V, but after that, there is a sharp decline and fluctuations lasting for 0.05 seconds. The steady-state voltage (158.5 V) has been adjusted to ensure alignment between text and illustration. Initially, the PV panel's power reached 220 W, but there were abrupt fluctuations before it stabilized at 250 W in 0.05 seconds. The analysis of fuel cell power, current and voltage is illustrated in Figure 9.

The fuel voltage graph is increased to reach 60, and the current value starts out at 280A before dropping to 1.5A in 0.025 seconds. 11KW of power is reached in 0.01 seconds. Figure 10 shows an examination of the battery's voltage, current, and SOC. SOC will be discharged to a final 99.7% after starting at 100%. At 0.05 seconds, when the battery is discharging, the Simulink voltage that the battery generates is 320 V. The battery's voltage rises to 450 V at first, then falls and rises once more to its steady-state condition. 1220 A is the starting battery current lowered to reach the steady-state. In the end, the SOC value is declining by 100%. The voltage of the source, injected present, and compensated voltage sag signals are examined sequentially in Figure 11.

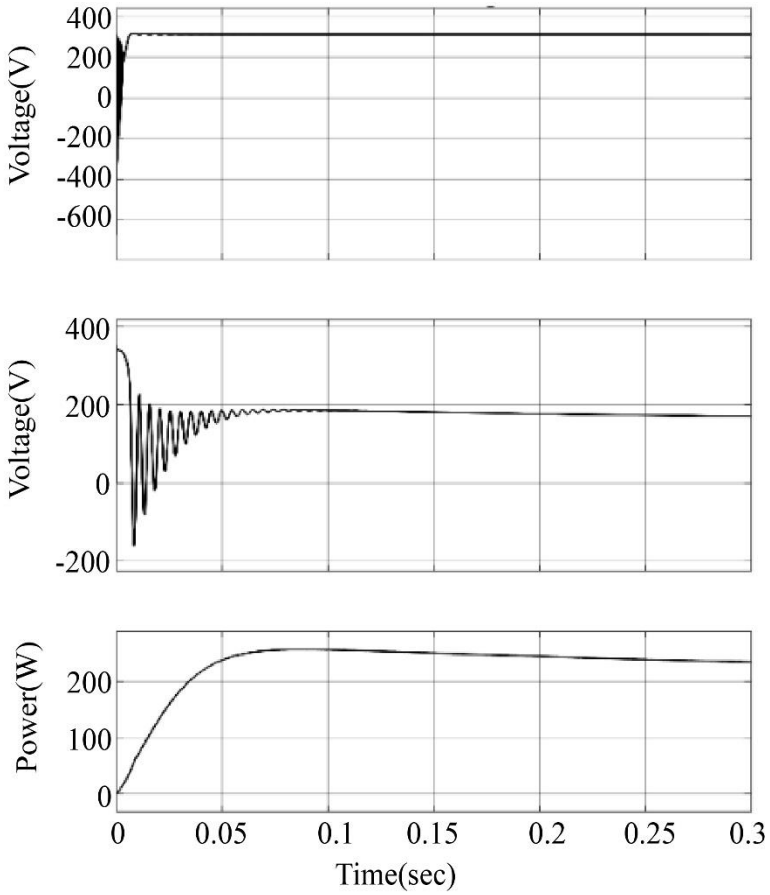

Fig. 8 PV System output power, voltage, and current

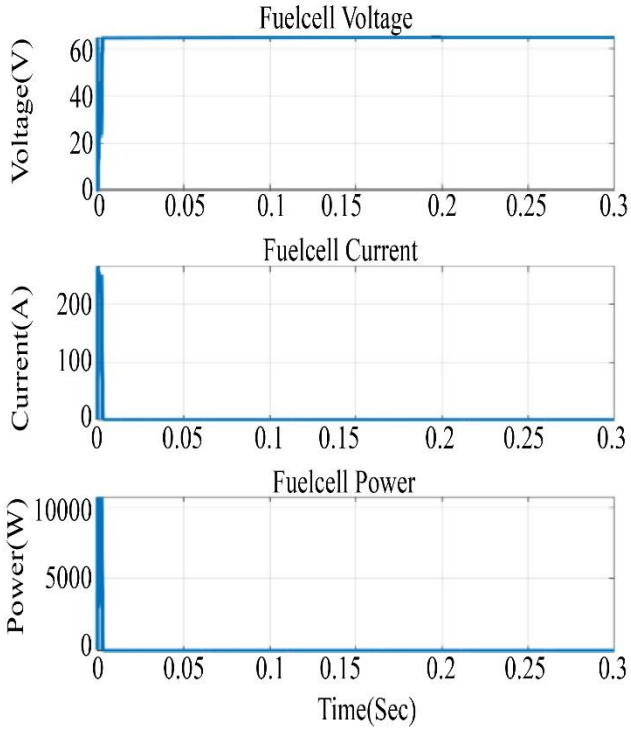

Fig. 9 Output of fuel cell voltage, current, and power

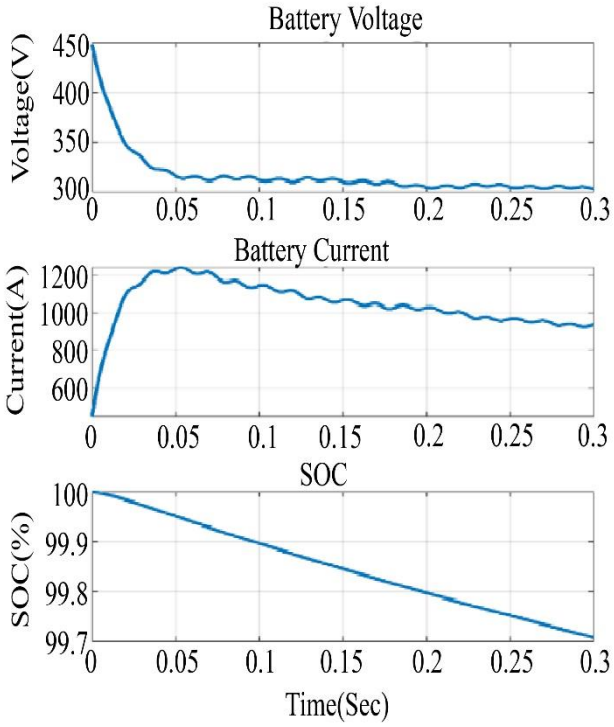

Fig. 10 Output of battery voltage, current, and SOC

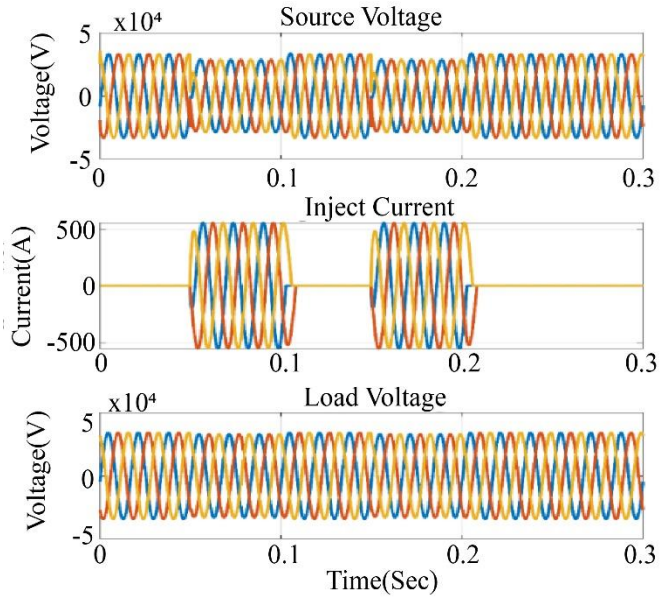

Fig. 11 Analysis of sag mitigation

A flaw in the interval of 0.05 to 0.2 seconds produces the source voltage. The source side's three-phase initial voltage is 3.5 kV. After 0.05 sec, it drops to 3.0 KV, and then it rains again for 0.1 sec to reach 3.5 kV. The STATCOM provides the injected current, which has a value of 520 A between 0.15 and 0.2 sec. The injected current, which is produced by the STATCOM between 0.15 and 0.2 seconds later, compensates for the compensated voltage. Figure 12 shows how the compensated sag signal for the proposed RNN-HHO IEEE 9 compares to standard RNN-HHO, conventional WOA, and EHO. The Algorithm for Whale Optimization (WOA) and Optimization of Elephant Herding (EHO) are widely used benchmark optimizers in swarm intelligence. WOA is a widely recognized algorithm that balances exploration-exploitation and is suitable for many problems. EHO, based on elephant herds' social behavior, is suitable for comparison in problems requiring intense exploitation and refinement. Both algorithms are accustomed to evaluating the suggested algorithm's robustness, scalability, and general applicability across AI-based optimization methods. Both algorithms are widely recognized and widely used in optimization research. The proposed approach mitigates the sag signal and settles it at 3.4 kV, so to correct the sag signal, 0.05–0.2 sec. The suggested WOA, RNN+HHO, and EHO methods of voltage sag mitigation are contrasted in the graph. The representation of time in seconds along the x-axis, and the voltage is illustrated on the y-axis. The voltage increases the value on the y-axis. As the graph demonstrates, the proposed strategy (blue line) is the most successful way to reduce voltage sag. It reduces voltage sag by up to 3.5 kV at 0.06 sec. EHO (purple line), RNN-HHO (red line), and WOA (yellow line) reduce voltage sag by up to 3.45 kV, 3.35 kV, and 3.32 kV, respectively. The proposed technique's sag compensation outperforms that of conventional methods. An analysis of the reduced voltage swell signal using STATCOM was presented in Figure 13.

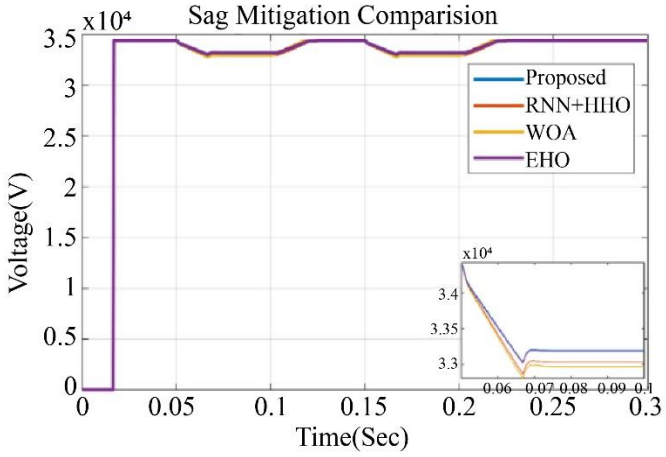

Fig. 12 Analysis of sag mitigation comparison

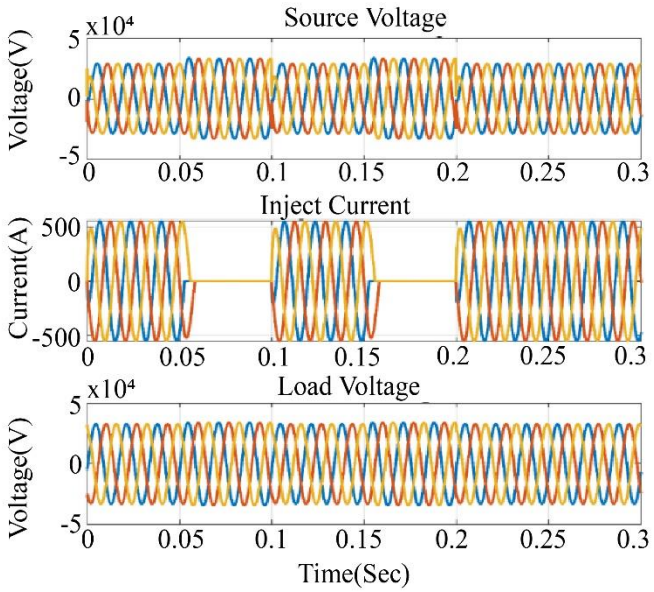

Fig. 13 Analysis of swell mitigation

This is a fault-created time interval where the swell signal overshoots from 3.5 kV at 0.05 sec to 0.2 sec. The current that is injected is also used through the STACTOM to make up for the swell indication, and at 3.5 kV, the compensated load voltage is finally achieved. Voltage swell mitigation and traditional methods are contrasted in Figure 14. The proposed technique (RNN-HHO+ IEEE 9) outperforms the conventional RNN-HHO, WOA, and EHO. The proposed RNN+HHO, WOA, and EHO methods of voltage swell mitigation are contrasted in the graph. The representation of time in seconds on the x-axis, and voltage is illustrated on the y-axis. The proposed strategy (blue line) is the most successful way to reduce voltage swell, as it reduces voltage swell by up to 3.55 kV at 0.1 sec. EHO (purple line), RNN-HHO (red line), and WOA (yellow line) reduce voltage swell by up to 3.35 kV, 3.33 kV, and 3.32 kV, respectively. The WOA and EHO are significantly more amplified than the swell signal. The specific time interval is magnified to further notice the suggested method's effectiveness. Figure 15 analyzes the voltage condition fluctuation, the current of injection, the load, and the source electricity. The source voltage reached 3.5 KV, and fluctuations are produced between 0.05 to 0.1 sec and 0.15 to 0.2 sec intervals. After that, the injected current, which is 520 A from 0.05 to 0.1 sec and 0.15 to 0.2 sec, is used by the STATCOM to make up the difference. It then rises and fluctuates until 0.3 sec.

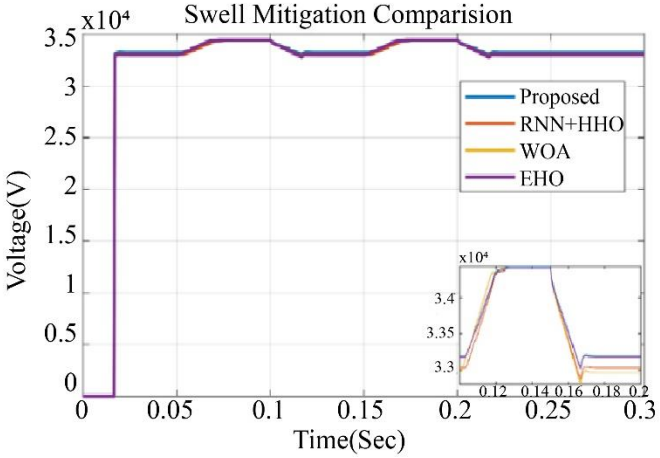

Fig. 14 Analysis of swell mitigation comparison

This injects current to balance the voltage on the load side. However, the load voltage stabilizes at 3.5 kV. A comparison of current techniques and voltage fluctuation reduction is shown in Figure 16. The proposed method (RNN-HHO+ IEEE 9) outperforms the WOA and EHO, as this graph makes evident. The proposed RNN+HHO, WOA, and EHO methods of voltage fluctuation mitigation are contrasted in the graph. The proposed strategy (blue line) is the most successful

way to reduce fluctuation, as it reduces voltage fluctuation by up to 3.45 kV at 0.1 sec. EHO (purple line), RNN-HHO (red line), and WOA (yellow line) reduce fluctuation by up to 3.34 kV, 3.33 kV, and 3.32 kV, respectively. The signal fluctuation is significantly reduced compared to the traditional RNN-HHO, WOA, and EHO. Moreover, the time span is specifically enlarged to demonstrate the superiority of the suggested approach. A power loss analysis is displayed in Figure 17. The proposed method (RNN-HHO+ IEEE 9) has a lower power loss than existing methods.

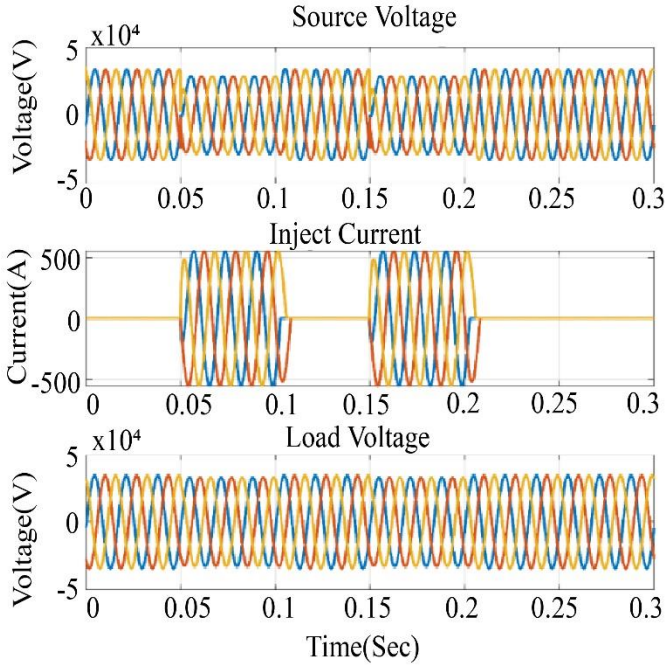

Fig. 15 Analysis of fluctuation mitigation

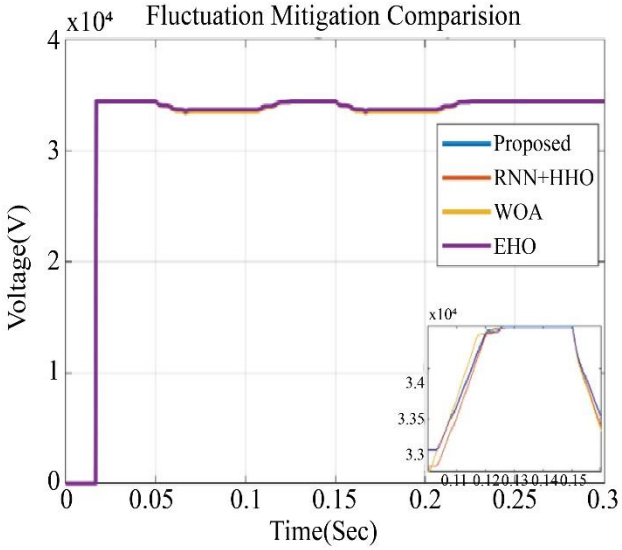

Fig. 16 Analysis of fluctuation mitigation comparison

Table 4. Comparison of THD existing approaches

Approaches	THD %
Proposed	1.114%
RNN-HHO	1.57 %
EHO	3.23 %
WOA	2.38 %

The cost comparison analysis is displayed in Figure 18. Compared to other current methods, including WOA and EHO, the proposed method (RNN-HHO+ IEEE 9) is less expensive. The suggested method's THD, combined with the methods of control, is shown in Figure 19.

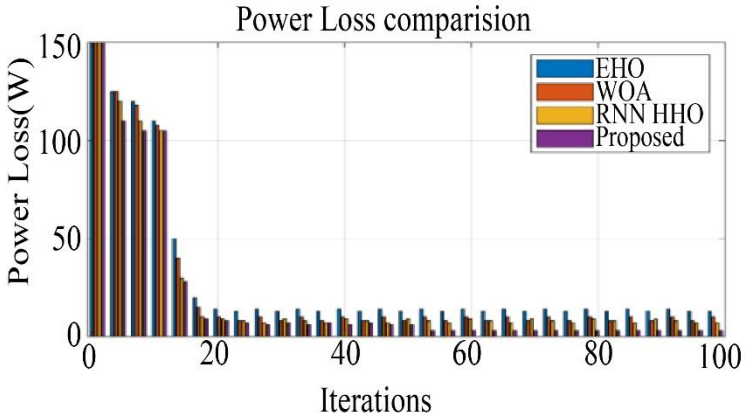

Fig. 17 Analysis of power loss comparison

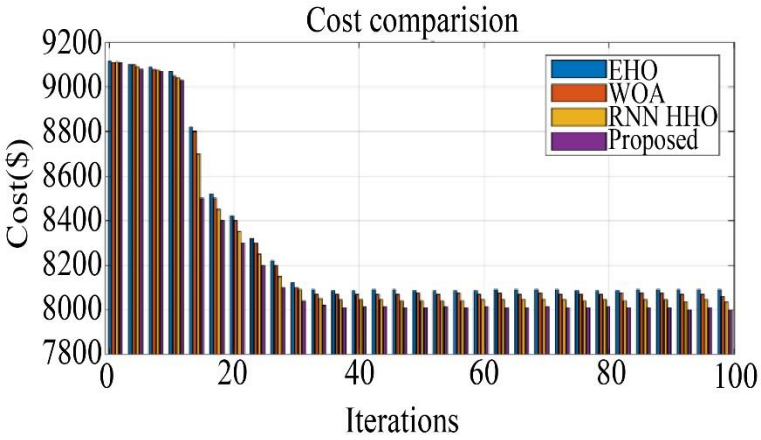

Fig. 18 Cost comparison

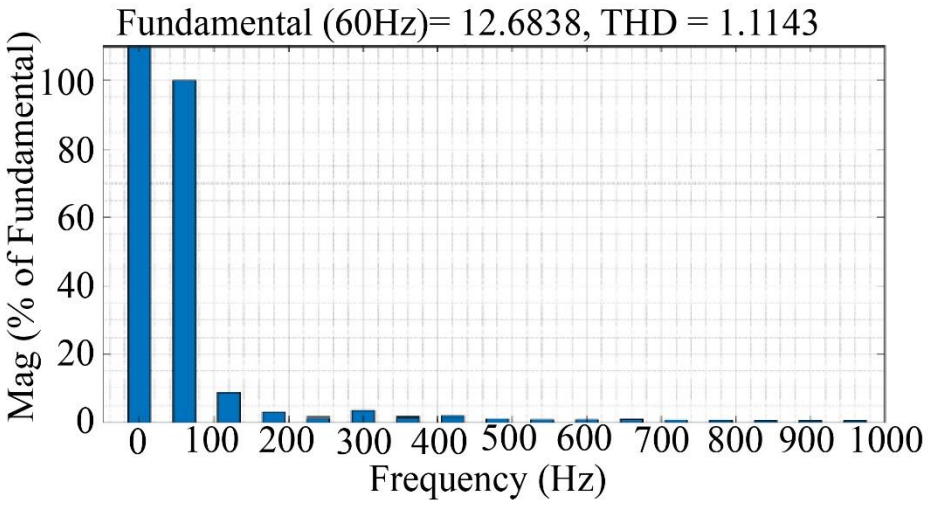

Fig. 19 THD comparison

The harmonic mitigation in this Figure is 1.114% relative to the frequency of 60 Hz. Furthermore, it is well known that the IEEE 9 RNN-HHO technique included in the proposed STATCOM is superior to the current standard RNN-HHO, WOA, and EHO techniques. This STATCOM RNNO-HHO and IEEE-9 system of buses significantly reduces the strength quality issues. A comparison of the THD percentage using conventional techniques is shown in Table 4. The THD percentages for the RNN-HHO, WOA, and EHO techniques are 1.57%, 2.38%, and 3.23%, respectively, making it abundantly evident that the proposed technique is superior to the traditional approaches.

5. Discussion

The paper evaluates the RNN-HHO approach's effectiveness in improving power quality in an HRES using an IEEE 9 bus architecture. The research simulated components and the STATCOM, the optimal controller, in MATLAB/Simulink. The RNN-HHO technique outperformed traditional methods, leading to a lower THD and stronger appearance in mitigating variations in voltage.

6. Conclusion

This proposed work provided a thorough modelling approach for HRES and assessed the system's improved operating limits after incorporating STATCOM. The main goal is to use a hybrid optimization strategy combining the advantages of RNN and HHO to augment the criteria for gaining PID Controllers inside the circuit for STATCOM control. The purpose of the proposed RNN-HHO optimization is to develop the overall system response to the inherent irregularities in HRES as well as voltage stability. To validate the performance of the combined RNN-HHO approach, it is implemented in MATLAB/Simulink 2020Ra and examined on a system with an IEEE 9 bus. Analysis is done on important performance metrics like voltage sag, swell, fluctuation, power loss, cost, and THD. The findings show that in terms of reducing PQ problems, the proposed RNN-HHO optimized STATCOM performs noticeably better than traditional controllers like WOA and EHO. More specifically, the proposed strategy reduces harmonics more effectively than RNN-HHO, WOA, and EHO, with a THD of 1.114% as opposed to 1.57% for RNN-HHO, 2.38% for WOA, and 3.23% for EHO. The investigation concludes that improving the stability and performance of HRES involves integrating STATCOM and an optimized control strategy that makes use of RNN-HHO in the bus system of IEEE 9. The suggested strategy reduces power loss and costs while mitigating PQ issues, making it a workable option for contemporary power systems with significant replenishable energy penetration. To deal with limitations on scaling and suggest further research on RNN-HHO optimized STATCOM for larger power systems and potential algorithm improvements.

References

[1] Darioush Razmi et al., "An Overview of Power Quality Issues and Control Strategies for Distribution Networks in the Presence of Distributed Generation Resources," *IEEE Access*, vol. 11, pp. 10308-10325, 2023. [CrossRef] [Google Scholar] [Publisher Link]

[2] Ndamulelo Tshivhase, Ali N. Hasan, and Thokozani Shongwe, "An Average Voltage Approach to Control Energy Storage Devices and Tap-Changing Transformers Under High Distributed Generation," *IEEE Access*, vol. 9, pp. 108731-108753, 2021. [CrossRef] [Google Scholar] [Publisher Link]

[3] Maria Tariq, Hina Zaheer, and Tahir Mahmood, "Modeling and Analysis of STATCOM for Renewable Energy Farm to Improve Power Quality and Reactive Power Compensation," *Engineering Proceedings*, vol. 12, no. 1, pp. 1-4, 2021. [CrossRef] [Google Scholar] [Publisher Link]

[4] Moses Jeremiah Barasa Kabeyi, and Oludolapo Akanni Olanrewaju, "Sustainable Energy Transition for Renewable and Low-Carbon Grid Electricity Generation and Supply," *Frontiers in Energy Research*, vol. 9, pp. 1-45, 2022. [CrossRef] [Google Scholar] [Publisher Link]

[5] Thamatapu Eswara Rao et al., "Performance Improvement of Grid-Interfaced Hybrid System Using Distributed Power Flow Controller Optimization Techniques," *IEEE Access*, vol. 10, pp. 12742-12752, 2022. [CrossRef] [Google Scholar] [Publisher Link]

[6] Gundala Srinivasa Rao, B. Srikanth Goud, and Ch. Rami Reddy, "Power Quality Improvement using ASO Technique," *2021 9th International Conference on Smart Grid (icSmartGrid)*, Setubal, Portugal, pp. 238-242, 2021. [CrossRef] [Google Scholar] [Publisher Link]

[7] B. Srikanth Goud, and B. Loveswara Rao, "Power Quality Improvement in Hybrid Renewable Energy Source Grid-Connected System using Grey Wolf Optimization," *International Journal of Renewable Energy Research-IJRER*, vol. 10, no. 3, pp. 1264-1276, 2020. [CrossRef] [Google Scholar] [Publisher Link]

[8] Adel Ab-BelKhair, Javad Rahebi, and Abdulbaset Abdulhamed Mohamed Nureddin, "A Study of Deep Neural Network Controller-Based Power Quality Improvement of Hybrid Pv/Wind Systems By Using Smart Inverter," *International Journal of Photoenergy*, vol. 2020, no. 1, pp. 1-22, 2020. [CrossRef] [Google Scholar] [Publisher Link]

[9] Muhammad Majid Gulzar et al., "An Innovative Converterless Solar Pv Control Strategy for A Grid-Connected Hybrid Pv/Wind/Fuel-Cell System Coupled Battery Energy Storage," *IEEE Access*, vol. 11, pp. 23245-23259, 2023. [CrossRef] [Google Scholar] [Publisher Link]

[10] Naeem Abas et al., "Power Quality Improvement Using Dynamic Voltage Restorer," *IEEE Access*, vol. 8, pp. 164325-164339, 2020. [CrossRef] [Google Scholar] [Publisher Link]

[11] T. Anuradha Devi et al., "Hybrid Optimal-FOPID based UPQC for Reducing Harmonics and Compensating Load Power in Renewable Energy Sources Grid-Connected System," *Plos One*, vol. 19, no. 5, pp. 1-53, 2024. [CrossRef] [Google Scholar] [Publisher Link]

[12] Nagwa F. Ibrahim et al., "Operation of Grid-Connected PV System ANN-based MPPT and An Optimized LCL Filter using GRG Algorithm for Enhanced Power Quality," *IEEE Access*, vol. 11, pp. 106859-106876, 2023. [CrossRef] [Google Scholar] [Publisher Link]

[13] S.N.V. Bramareswara Rao et al., "An Adaptive Neuro-Fuzzy Control Strategy for Improved Power Quality in Multi-Microgrid Clusters," *IEEE Access*, vol. 10, pp. 128007-128021, 2022. [CrossRef] [Google Scholar] [Publisher Link]

[14] Komal Mehra, Gursewak Singh Brar , and Ranvir Kaur, "Power Quality Improvement using DSTATCOM for IEEE 9 Bus System," *International Journal of Innovative Research in Computer Science and Technology*, vol. 10, no. 5, pp. 113-118, 2022. [Publisher Link]

[15] Mohamed I. Mosaad et al., "Near-Optimal PI Controllers of STATCOM for Efficient Hybrid Renewable Power System," *IEEE Access*, vol. 9, pp. 34119-34130, 2021. [CrossRef] [Google Scholar] [Publisher Link]

[16] D.Dhana Prasad et al., "Power Quality Improvement in WECS using ANN-STATCOM," *International Journal for Modern Trends in Science and Technology*, vol. 7, no. 7, pp. 160-165, 2021. [Google Scholar] [Publisher Link]

[17] Atma Ram, Parsh Ram Sharma, and Rajesh Kumar Ahuja, "Enhancement of Power Quality using U-SOGI-based Control Algorithm for DSTATCOM," *Ain Shams Engineering Journal*, vol. 15, no. 1, pp. 1-20, 2024. [CrossRef] [Google Scholar] [Publisher Link]

[18] Sachin Kumar, Akhil Gupta, and Ranjit Kumar Bindal, "Power Quality Investigation of a Grid-Tied Hybrid Energy System using a D-STATCOM Control and Grasshopper Optimization Technique," *Results in Control and Optimization*, vol. 14, pp. 1-12, 2024. [CrossRef] [Google Scholar] [Publisher Link]

[19] Mohit Bajaj et al., "Power Quality Assessment of Distorted Distribution Networks Incorporating Renewable Distributed Generation Systems Based on the Analytic Hierarchy Process," *IEEE Access*, vol. 8, pp. 145713-145737, 2020. [CrossRef] [Google Scholar] [Publisher Link]

[20] Ramchandra Adware, and Vinod Chandrakar, "Power Quality Enhancement in a Wind Farm Connected to a Grid with a Fuzzy-Based STATCOM," *Engineering, Technology & Applied Science Research*, vol. 13, no. 1, pp. 10021-10026, 2023. [CrossRef] [Google Scholar] [Publisher Link]

[21] Hatem F. Sindi et al., "Robust Control of Adaptive Power Quality Compensator in Multi-Microgrids for Power Quality Enhancement Using Puzzle Optimization Algorithm," *Ain Shams Engineering Journal*, vol. 14, no. 8, pp. 1-18, 2023. [CrossRef] [Google Scholar] [Publisher Link]

[22] Saeed Hasanzadeh et al., "Power Quality Enhancement of the Distribution Network by Multilevel Statcom-Compensated based on Improved One-Cycle Controller," *IEEE Access*, vol. 10, pp. 50578-50588, 2022. [CrossRef] [Google Scholar] [Publisher Link]

[23] B. Srikanth Goud et al., "Power Quality Improvement using Distributed Power Flow Controller BWO-based FOPID Controller," *Sustainability*, vol. 13, no. 20, pp. 1-33, 2021. [CrossRef] [Google Scholar] [Publisher Link]

[24] Noor Zanib et al., "Performance Analysis of Renewable Energy-based Distributed Generation System using ANN Tuned UPQC," *IEEE Access*, vol. 10, pp. 110034-110049, 2022. [CrossRef] [Google Scholar] [Publisher Link]

[25] B. Srikanth Goud et al., "PV/WT Integrated System using the Grey Wolf Optimization Technique for Power Quality Improvement," *Frontiers in Energy Research*, vol. 10, pp. 1-14, 2022. [CrossRef] [Google Scholar] [Publisher Link]

[26] Omar Makram Kamel et al., "A Novel Hybrid Ant Colony-Particle Swarm Optimization Techniques based Tuning STATCOM for Grid Code Compliance," *IEEE Access*, vol. 8, pp. 41566-41587, 2020. [CrossRef] [Google Scholar] [Publisher Link]

[27] Vijoy Kumar Peddiny, Brajagopal Datta, and Abhik Banerjee, "Performance Improvement of Combined Wind Farms using ANN-based STATCOM and Grey Wolf Optimization-based Tuning," *Journal of Operation and Automation in Power Engineering*, vol. 13, no. 3, pp. 248-254, 2024. [CrossRef] [Google Scholar] [Publisher Link]

[28] Alok Kumar Mishra et al., "PSO-GWO Optimized Fractional Order PID based Hybrid Shunt Active Power Filter for Power Quality Improvements," *IEEE Access*, vol. 8, pp. 74497-74512, 2020. [CrossRef] [Google Scholar] [Publisher Link]

[29] Ali Moghassemi et al., "A Novel Solar Photovoltaic Fed TransZSI-DVR for Power Quality Improvement of Grid-Connected PV Systems," *IEEE Access*, vol. 9, pp. 7263-7279, 2020. [CrossRef] [Google Scholar] [Publisher Link]

[30] Srishail K. Bilgundi et al., "Grid Power Quality Enhancement using An ANFIS Optimized PI Controller for DG," *Protection and Control of Modern Power Systems*, vol. 7, no. 1, pp. 1-14, 2022. [CrossRef] [Google Scholar] [Publisher Link]

[31] Muhammed F. Alwaeli, Sadjad Galvani, and Vahid Talavat, "Addressing Power Quality Challenges in Hybrid Renewable Energy Systems through STATCOM Devices and Advanced Grey Wolf Optimization Technique," *Results in Engineering*, vol. 25, pp. 1-13, 2025. [CrossRef] [Google Scholar] [Publisher Link]

[32] Marwa Ben Slimene, and Mohamed Arbi Khlifi, "A Hybrid Renewable Energy System with Advanced Control Strategies for Improved Grid Stability and Power Quality," *Scientific Reports*, vol. 15, no. 1, pp. 1-18, 2025. [CrossRef] [Google Scholar] [Publisher Link]